

Water Quality Sensors for Smart Cities

Alan Mickelson

University of Colorado at Boulder
1111 Engineering Drive
Boulder, Colorado 80309-0425
mickel@colorado.edu

Daniel Tsvankin

Department of Mechanical Engineering
1111 Engineering Drive
Boulder, Colorado 80309-0427

ABSTRACT

The use of water quality sensors for the prediction of the coupling of urban food, energy and water (FEW) subsystems is discussed. A high level model of FEW coupling is presented. The role of fine grained sensing in determination of system coupling is introduced. An archetypical water quality sensing element is demonstrated and calibrated. A physical model for an environmentally stressed water system is presented. Sensor calibration data is applied to the problem of using an array of water quality sensors for determining system stressors and thereby FEW couplings. The requirements for resource management derived from smart city control system data and FEW system coupling is discussed.

KEYWORDS

computers, sensors, monitoring, modeling

ACM Reference format:

Alan Mickelson and Daniel Tsvankin. 2017. Water Quality Sensors for Smart Cities. In *Proceedings of International Conference on Smart Digital Environment, Rabat, Morocco, July 21 - 23, 2017 (ICSDE'17)*, 8 pages.
<https://doi.org/10.1145/3128128.3129386>

1 INTRODUCTION

Advances in communication and computer technology are heralding an era where an urban environment can offer quality of life as well as economy of scale. High population density minimizes resource use for housing yet traditionally has caused distribution bottlenecks as evidenced by city traffic. Distribution of energy and water resources across a population is facilitated by density of housing yet unequal distribution of resources in urban environments results in heterogeneous distribution of wealth between urban neighborhoods. Urban environments often have precluded food production within the urban boundaries. Unabated growth drives up suburban land price precluding traditional food production in areas even near urban boundaries. Smart city

Permission to make digital or hard copies of all or part of this work for personal or classroom use is granted without fee provided that copies are not made or distributed for profit or commercial advantage and that copies bear this notice and the full citation on the first page. Copyrights for components of this work owned by others than ACM must be honored. Abstracting with credit is permitted. To copy otherwise, or republish, to post on servers or to redistribute to lists, requires prior specific permission and/or a fee. Request permissions from permissions@acm.org.

ICSDE'17, July 21 - 23, 2017, Rabat, Morocco
© 2017 Association for Computing Machinery.
ACM ISBN 978-1-4503-5281-9/17/07...\$15.00
<https://doi.org/10.1145/3128128.3129386>

technology combined with food, energy and water management awareness can result in cities that can produce food locally without affecting energy production and distribution and while preserving water quality.

Coupling between food, energy and water distribution systems are inextricably intertwined in communities of any size from a shanty in Baja California to a mega city in China [14, 18, 21, 24]. Smart technology tends to focus on a single subsystem at a time, for example, a smart grid [13, 15] or a smart farm [10, 20, 32, 33, 36, 41]. Water quality, however, is affected by each of the FEW (food, energy and water) [11, 17, 43, 44] subsystems. Smart city management will require real time resource management decisions to occur both automatically and manually. In the present work, it is hypothesized that the water quality monitoring can be used to determine couplings between FEW subsystems as well as to determine magnitude and location of FEW stressors [11, 25, 26].

Fine grained spatial distribution of sensors require low cost and autonomy of operation, that is, the sensors should be able to function without external power source and store data until interrogation. Important interactions between food production and water involve the release of nitrogen (nitrate) and phosphorous (phosphates) into the water system that subsequently can lead to eutrophication [6, 7, 9, 22, 23, 34, 35]. Eutrophication has a serious affect on oxygen content of water. Important interactions between energy production and water involve the release of pollutants and heat that affect dissolved solids, turbidity and temperature.

In the present work, a high level, predictive model of a FEW system developed in a separate work [26] is briefly presented. The roles of coarse grain and fine grain measurements are elucidated. An archetypical micro-controlled sensor element that includes five sensing elements is demonstrated. The parameters sensed are temperature, pH, turbidity, nitrate and dissolved oxygen. A model for an environmentally stressed water system is presented. The efficacy of a system of sensor elements for determining system stressors is considered in light of calibration data taken on the demonstrated sensing element. Requirements for data to be used in prediction of the dynamics of a FEW system are discussed.

2 MODELING FEW SYSTEMS

Although details of a high level model have been submitted elsewhere [26], certain details of the approach are presented here in this section in order to make this presentation as self-contained as feasible in a conference proceeding. Here, the goal is to find as simple a system as can exhibit real

behavior, that is, behavior that corresponds at least to the simplest of community ecosystems. The goal is to understand the requirements that the model places on the sensors and control system. Evidently, the more abstract a system model is used, the more simple the representation can be. Coarse grained representations of the food, energy and water supply quantities are used at the highest level in order to exhibit trade-offs between the subsystems. More fine grained models are necessary to quantify the food and water subsystems. In particular, we discuss what a spatial temporal flow model would look like. This model is an archetype for the water quality models that can use sensor data as input to determine stressor location and dynamical behavior.

The simplest way to analyze an essentially nonlinear system is to identify a stable point and expand for small deviations of the variables about that point. Here we will define our primary variables as functions of time only. These variables will be the total supply of food, power and water. We will assume that there is a stable state in which there is constant total output of each of our variables. That is, if the integrated food, power and water demand were constant, we could write that

$$\frac{d\mathbf{V}(t)}{dt} = 0 \quad (1)$$

where \mathbf{V} is a three component (abstract) vector with components $V_1(t) = V_F(t) - V_F(0)$, $V_2(t) = V_E(t) - V_E(0)$ and $V_3 = V_W(t) - V_W(0)$, where the $V_i(t)$ are the integrated available food, power and water. The $V_i(t)$ where $i = 1, 2, 3$ are zero mean quantities and the V_i where $i = F, E, W$ are quantities with magnitudes (and dimensions) that really correspond the total of subsystem's supply. Quantifying what is meant by the total supply of food is somewhat of a task in that there are many types of food and many ways to categorize food (kcal/mole for example). That this can be done in the case of a community with a single staple such as rice heartens us that there is a way to make this definition. For power (energy), the process is much simpler. The total power would be the total of all of the power drawn from the electrical grid at a given time. Just as the total power would be a sum of all of the power drawn from a number of tap points, the food total is a sum of quantities of food procured at distribution points. The total water would be the total that was drawn from all of the taps, spigots, etc at a given time.

The demand for food, power and water is not constant during an hour, a day or a week. There is a demand function $D_i(t)$ where $i = 1, 2, 3$ that determines this demand. This function really needs to be measured for a given community and then fit for diurnal as well as seasonal, annual and longer cycles. These temporal patterns can then be used as drivers. Of course, if the generation $G_i(t)$ minus the system loss $L_i(t)$ of each of the V_i were to exactly follow the demand, then the equilibrium could be maintained. In general, though, we need to write

$$\frac{d\mathbf{V}(t)}{dt} = \mathbf{G}(\mathbf{V}; t) - \mathbf{L}(\mathbf{V}; t) - \mathbf{D}(t) \quad (2)$$

where here the $(\mathbf{V}; t)$ has been included in the argument of the generation and loss functions to indicate that generation of food requires power and water just as the generation of power and water require water and power. This use of power and water in the generation function needs to be accounted for in the loss functions.

We have not tracked in our system, though, the wastewater nor the water quality of the fresh surface water. A separate account of water could be made by considering the initial quantity of freshwater water input to the system and how this quantity varies as it propagates through the system. This would require defining a $V_W(\mathbf{r}, t)$ as a function of time and space, the space variable \mathbf{r} here consisting of three coordinates, one along the flow direction and two transverse to the direction of flow. The quantity input to system will separate into freshwater, wastewater and loss to the system as the initial quantity of freshwater flows through the system. This system can be described by a flow equation that will in general be of the form

$$\mathcal{N}\{V_W(\mathbf{r}, t)\} = L(\mathbf{r}, t) \quad (3)$$

where \mathcal{N} is an (in general non-linear) propagation operator (hydrodynamic equation of motion) that moves the freshwater through the system. The usual hydrodynamic operator is second order in space and then requires initial conditions on the quantity and flow at the input of the water supply system.

Contaminants to the system can be tracked also with a hydrodynamical model. Concentrations $C_i(\mathbf{r}, t)$ will flow through the system subject to augmentation by sources of pollutants such that

$$\mathcal{N}\{C_i(\mathbf{r}, t)\} = \sum_{j=1}^{N_s} S_{ij}(\mathbf{r} - \mathbf{r}_j, t) \quad (4)$$

where the $S_{ij}(\mathbf{r}, t)$ is the j^{th} source of the i^{th} contaminant located at the coordinate \mathbf{r}_j . These source locations and strengths are to be determined by the sensor network under discussion. It is these sources that determine the coupling of the other subsystems (food and energy) into the water subsystem. Knowledge of these sources is a necessary step in affecting solution to the nonlinear system of Eq. 1.

3 COARSE AND FINE GRAIN SENSING

Smart cities will require individual smart grids for food, energy and water as well as an integrated management system to carry out joint and coordinated control. A smart power grid, by nature, requires fine grain sensors, that is, localized sensors to make point measurements of voltage and current as a function of length along the associated transmission lines. Information about the state of voltage and current of power generating units that can be switched in and out of the main transmission line are also determined primarily by point measurements at the junctions where the switches are located. When the sources of power are heterogeneous, that is, include various renewables (solar, wind, geothermal) along

with more conventional sources (gas fired, hydro electric, nuclear), it is also necessary to know the detailed state of the sun, wind, earth at the time of the change of the mix of energy sources. This information is not necessarily fine grain but, again will be applied to the points where switches attach sources of voltage and current to the line. The sensing that goes into controlling the electric grid can be thought of as consisting of fine grain measurements even though the result of the control system is to produce an equilibrium over considerable lengths and times.

The availability of satellite imagery allows for collection of multitudes of coarse grain data for food [32, 33] and water systems [5–8, 16] at minimal cost. Image processing can be applied to convert imagery to control system data for coarse grained decision making. Images obtained on a daily basis can be used determine the colors of crops and how the colors change on the scale of days. Color change can be used as servo mechanism, for example, to determine when or how much to irrigate a given field in the context of smart agriculture. The color of the crops here would be determined from data obtained from multiple pixels with multiple wavelength data where those multiple pixels are an average over many plants. Fine grained control in the smart agricultural context might consist of a multitude of soil humidity sensors embedded in the ground between plants. The response time of such sensors is essentially instantaneous in comparison with daily image data. The fine grained data can be used to alter the rules for coarse grain analysis to reduce grid size near where higher resolution may be necessary. The fine grain data might also be used for plant by plant control of the water emanating from a drip irrigation system. This fine grain control is more complex than simply using fine grain data to augment coarse grain control although there may be great pay-off in crop yield. Some hybrid of the two approaches might be the most optimal.

Much as is the case with images of fields, ground water also appears on satellite and other areal imagery. Image processing of shores can be used to determine the relative quantity of water behind a dam. Color can be used to infer agitation or relative concentrations of pollutants. Multi-wavelength images yield information about differing depths through the wavelength dependence of the absorption coefficient. The wavelength dependence can also indicate the composition of dissolved solids in the water [4, 5]. But again, here, imagery averages over pixels and pixels are already averaged over distances depending on the remoteness of the recording cameras [19]. Fine grain sensors can be used to inform the coarse grain or to carry out fine grain control informed by the coarse grain [3, 12, 27].

As was hypothesized in [11], water quality is a good indicator of the coupling of the food, energy and water (FEW) subsystems. Although the FEW subsystems are always coupled, that coupling becomes especially noticeable in the presence of environmental stressors. This was mathematically expressed by the driving term on the right hand side of Eq.

4. Determination of the details of the driving term of Eq. 4 serves to inform the solution of the coupled FEW system.

4 SENSORS AND CALIBRATION

Water quality measurements have traditionally been painstaking [1, 26]. Sampling water at various spatial locations meant physically transporting sample containers to the point of measurement, transporting those containers back to a well-stocked laboratory and conducting detailed tests. Certain of water measurements, for example, direct measurements of heavy metal, still require laboratory tools such as mass spectrometers. Although multi-spectral techniques can be used wth remote imaging [2, 35], most satellite imagery is not multi-spectral. Advances in digital technology, though, led to great strides within the first decade of this millennium resulting in numerous demonstrations of water quality sensing networks [28, 29, 31, 37–40, 42].

Micro-controller technology for consumers has come a long way since 2007, in part due to the ubiquity of such controllers as the Arduino and, more recently, Raspberry Pi. Numerous read-out technologies are now possible [30, 43]. A package that contained sensors for temperature, pH, conductivity, total dissolved solids (TDS), dissolved oxygen and turbidity cost as much as \$3400 in 2009 [39]. Micro-Arduino components have allowed the packages to shrink in size and cost. Fig. 1 is a picture of a pH sensor with its associated control board. Fig. 2 is of a bread board mounted unit wired together in my laboratory here in Boulder, Colorado. Indeed, this board has taken the micro-Arduino based approach [25, 26, 30]. This realization of the five sensor unit (temperature, pH, turbidity (not attached at the time of the picture), nitrate and dissolved oxygen) demonstrates that the micro-Arduino is a unit smaller than the pH controller yet the micro-Arduino can be used to fully control all five sensors. In fact, the volume occupied by all of the control electronics is quite small compared to any of the sensor heads indicating that a quite compact package could be produced for the multi-element sensor if the sensor heads are to be free standing or separately housed.

Table 1 contains some of the salient features of a set of calibration measurements of the outputs of the sensor pack. The calibration measurements were made by shutting off the sensor for some period of time. The sensor was then reactivated with the head located in a fixed position in a solution whose composition and temperature had settled. Data was taken from that time forward. The micro-processor can sample at 10 ms intervals. The temperature is the only sensor output that stabilized in roughly this amount of time. That is, the temperature jumped from a single value well below the steady state of 23°C to a value that oscillated about this steady state. The other sensors were slow enough that the 10 ms intervals sampled a portion of an exponential rise or exponential decay to steady state. The oscillations about steady state for the digital temperature is about 1%. This could simply indicate that the last of the eight bits of the read-out is uncertain. Only the oxygen and nitrate



Figure 1: A picture of a pH sensor with control board. The sensor head is much larger than the board. The board can be replaced by a micro-controller no bigger than the board but capable of controlling and reading out a multitude similar sensors. The sensor can also be interrogated by a smart phone that already contains a programmable micro-controller.

quantity/sensor	cal val	settling time	precision
temperature	23° C	10 ms	1%
pH	6.7	20 s	1%
turbidity	2070 NTU	200 ms	1%
nitrate	7 mg/l	100 ms	3%
oxygen	4.5 mg/l	300 s	2%

Table 1: A table of values of the average values of the solution used in calibration, the settling times and the precisions for the five sensors included in the micro-Arduino water quality measurement pack developed and discussed in this paper. The settling time is an estimate of how long the measured data takes until the measured value is within the measured precision of the mean value.

read-outs exhibit slightly more than a one bit round off. This may be due to my own approximation that the curves are either rising (in the cases of temperature and pH) or dying (in the cases of turbidity, nitrate and oxygen) exponentials. If the fit is bad, then the standard deviation will look higher. Data curves appear elsewhere [25].

This method of calibration yields information that can be used to optimize operation. Battery life is crucial in autonomous operation. Given a battery pack and set of sensors, total energy per measurement cycle can be minimized by powering up sensors only during a measurement. Accurate measurement then requires that each sensor be on for at least a settling time. This leads to a power reduction strategy where some sensors must be turned on for many more measurement periods than others. A result of this is the data of Table 2. The turbidity sensor is not included in the five

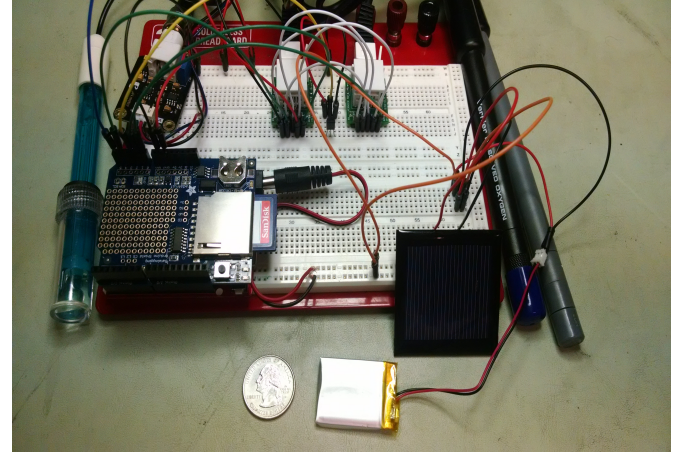


Figure 2: A picture of a micro-Arduino based, autonomous sensor package that includes commercial nitrate (Vernier NO3-BTA) and dissolved oxygen (Vernier DO-BTA) sensors along with the more usual water quality sensors (temperature, pH). The pH sensor (Robot Shop RB Dfr-483) element is a long cylindrical element as are the dissolved oxygen and pH sensor elements. The pH sensor element lies to the left of the board and the dissolved oxygen and pH are to the right with the dissolved oxygen closer to the board. The analog temperature sensor (Adafruit TMP-36), by contrast, is quite compact and lies between two couplers near the row to the back and column to the right of center. A turbidity sensor (GE 920-480A-E-LR) was not attached to the micro-Arduino board at the time of the picture. The micro-Arduino unit is coupled to the outside world with a class 1 bluetooth unit that can transmit over tens of meters.

sensors in this data set. Both the analog and digital temperature sensors were included bringing the total number of sensors plugged into the micro-Arduino to five. The table lists the amperage drawn by each sensor as a percentage of the total amperage drawn by all of the sensors (when they

sensor/power	temp(a)	temp(d)	pH	NO ₃	O ₂
% average	0%	5%	40%	40%	15%
% energy	0%	0%	3%	2%	95%

Table 2: A table indicating the percentage of current drawn by each sensor of the sensors in a package that includes analog and digital temperature, pH, nitrate and dissolved oxygen sensors when they are activated simultaneously in one column and the percentage of total energy expended by each during a cycle of measurement when each sensor is turned on only so long as to settle to a reliable measurement value.

are all turned on) in one column and the energy (amperage corrected for the settling time of the sensor) as a percentage of the total energy needed to complete the five measurements.

Although pH and nitrate both draw significantly more current than the others, the excessively long settling time of the dissolved oxygen sensor would cause this sensor to consume almost all the battery power were these the five sensors chosen for an autonomous package. Needless to say, these five sensors would not be good choice for an autonomous package both because of the poorly matched powers and the poorly matched on times. The calibration data, though, is not the only consideration in choosing a measurement set as we will see in the next section where we consider what data we really need to extract from the sensor package in order to determine the coupling between FEW subsystems.

5 STRESSORS AND DIFFUSION

Placement of an array of autonomous water quality sensors throughout a region of interest on the surface of a body of water and continuous monitoring of the output of the array will record the concentrations $C_i(\mathbf{r}, t)$ that appear in Eq. 4. If the sensor locations and their time records were continua, singularities of the $C_i(\mathbf{r}, t)$ would indicate source locations of the contaminant i . The finite number of sensors and their limited response time will determine the accuracy with which number of stressors and the stressor locations can be determined.

In order to ascertain what can be determined about stressors using an array of sensing elements that each contains the five previously discussed sensors (digital temperature, pH, nitrate, turbidity and dissolved oxygen), we consider a regular array of such elements placed on a homogeneous fluid that is subject to point perturbations of temperature, pH, nitrate, turbidity and oxygen. Applying a point source of material to a point on the surface of a fluid will generally give rise to a convective flow that is a combination of advection due to existing currents along with currents generated by the injection, coupled with diffusion of the particles that make up the contaminant. For the present discussion, we ignore the effect of advection. The complexities of hydrodynamic flow are beyond the scope of this presentation. The time and length scales of the diffusive flow contain meaningful information concerning the source determination problem even in the presence of advection. Later we will discuss how we could additively include water currents into the picture were the body of interest a stream or river.

We will assume that a stressor is applied at the point (x_s, y_s) on the surface ($z=0$) of the body of water that we characterize by an (x, y, z) coordinate system. We assume that the z -directed diffusion has a minimal effect on the two-dimensional problem (for whatever reason). This allows us to describe the diffusant concentration with the two-dimensional diffusion equation

$$\frac{\partial \psi(x, y, t)}{\partial t} - D \frac{\partial^2 \psi(x, y, t)}{\partial x^2} - D \frac{\partial^2 \psi(x, y, t)}{\partial y^2} = \delta(x - x_s, y - y_s) f(t) \quad (5)$$

where the two-dimensional delta function at coordinate (x_s, y_s) is the embodiment of the point source and the $f(t)$ is the

temporal driving function. The $\psi(x, y, t)$ of Eq. 5 can be identified with the $S_{ij}(\mathbf{r}, t)$ of Eq. 4 any one of the diffusants i located at a single point \mathbf{r}_s . Mathematically, that can be stated as

$$\psi(x, y, t) = S_{ij}(\mathbf{r} - \mathbf{r}_j) \delta_{js} \quad (6)$$

for one of the i 's. The general solution of Eq. 5 is given by

$$\psi(x, y, t) =$$

$$\frac{1}{4\pi t} \int_0^t \exp \left[- \left(\frac{(x - x_s)^2 + (y - y_s)^2}{4Dt'} \right) \right] f(t') dt' \quad (7)$$

To discuss applications, we need to consider scale in more detail. The extent of the water resource we are considering is order of tens of meters to a few kilometers. Diffusion constants are available from many sources. Heat (and resulting temperature change) diffuses relatively slowly in de-ionized water at 25° , on the order of $2.5 \times 10^{-2} \text{ cm}^2/\text{s}$. However, impurities in water raise this value into the range of tens of cm^2/s for even rather pure drinking water. pH and turbidity diffusion will depend on the diffusant. pH is most affected by strong bases such as ammonia and/or strong acids such as sulfur acid. Ammonia diffuses at a rate of $19.7 \text{ cm}^2/\text{s}$ and sulfate at a rate of $10.6 \text{ cm}^2/\text{s}$. Hydrogen phosphate is slightly lower at a rate of $7.6 \text{ cm}^2/\text{s}$ where oxygen is higher again at a rate of $20 \text{ cm}^2/\text{s}$. We see a pattern emerging in which most of the diffusants we consider diffuse at rates around $10 \text{ cm}^2/\text{s}$. The spread of turbidity depends on the cause of the turbidity but for simplicity can be assumed to be in a comparable range.

Fig. 3 illustrates a one-dimensional trace of the spatial distribution of diffusants about a source point at various

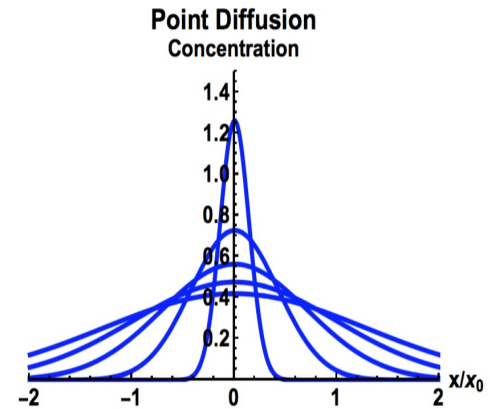


Figure 3: Spatial distribution of a diffusant for five different (dimensionless) times $t/t_0=0.2, 0.6, 1.0, 1.4, 1.8$ (from highest peaked density to smoothest) after a point impulse (magnitude ψ_0) of the diffusant is applied at the origin of the $(x/x_0=0)$ coordinate system.

times after the application of an impulse. We write the dimensionless time as t/t_0 and the dimensionless distance by x/x_0 . The $t_0=x_0/\sqrt{4D}$ where the x_0 is a free parameter that

can be chosen to represent the length scale of interest. We can choose our scale of interest by virtue of the diffusion dynamics only being dependent of the dimensionless constant $x/\sqrt{4Dt}$. The horizontal axis is x/x_0 and the times $t/t_0=0.2, 0.6, 1.0, 1.4, 1.8$ in Fig. 3. An expression for this one-dimension concentration function is

$$\psi(x, t) = \frac{1}{\sqrt{4Dt}} \exp \left[-\frac{x^2}{4Dt} \right]. \quad (8)$$

We note that the $\psi(x, t)$ has dimensions of per length if ψ_0 is dimensionless (ψ_0 , for example, representing the number of particles in the impulse). The concentration is very high for small times.

In Fig. 4, the concentration is plotted as a function of (dimensionless) time t/t_0 for fixed points (0.2, 0.6, 1.0, 1.4,

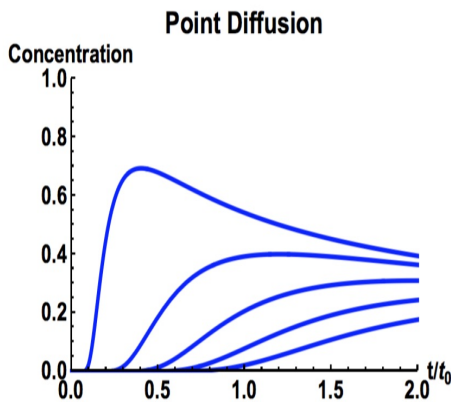


Figure 4: Time evolution of diffusing concentration at five different fixed distances from the point at which an impulse of diffusant is applied. The distances to the observation point along the x/x_0 axis are given by $x/x_0=0.2, 0.6, 1.0, 1.4$ and 1.8 from the sharpest to the smoothest distribution.

1.8) along the dimensionless (x/x_0)-axis. We see here that there the $1/e$ point of the concentration passes a given x/x_0 coordinate at a dimensionless time t/t_0 equal to that x/x_0 value. Were we to take the diffusion constant to be $7 \text{ cm}^2/\text{s}$, the rate of motion of the $1/e$ point would be of order 3 m in an hour.

When the source is considered as point-like but constant in time, we can also also write down an analytical expression for the concentration as a function of the dimensionless constant $x/\sqrt{4Dt}$ as

$$\psi(x, t)/\psi_0 = \operatorname{erfc} \left[\frac{x}{\sqrt{4Dt}} \right] \quad (9)$$

where erfc is the complementary error function that is defined in terms of the integral

$$\operatorname{erfc}(x) = \frac{2}{\sqrt{\pi}} \int_x^\infty \exp(-q^2) dq \quad (10)$$

that is, an integral over the the fundamental solution of Eq. 8. One would expect this to be the case given the Green's function solution of Eq. 7. In this constant source case, the source can be normalized and only the shape of the distribution changes as one would expect for a constant source as is seen in Fig. 5. The constancy of the peak indicates that the source is tacitly assumed to be injecting diffusant at the rate

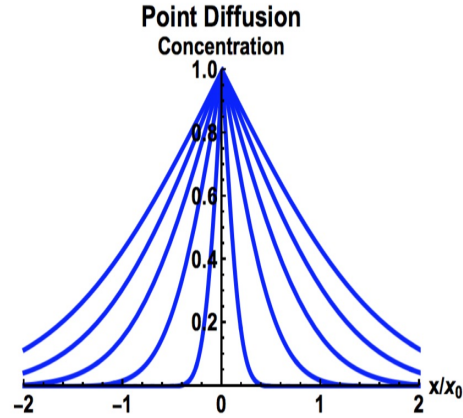


Figure 5: Spatial distribution of a diffusants for five different (dimensionless) times $t/t_0=0.2, 0.6, 1.0, 1.4, 1.8$ (from highest peaked density to smoothest) after a constant source (magnitude ψ_0) of the diffusant is attached at the origin of the ($x/x_0 = 0$) coordinate system.

that the material is moving away from the source volume. In this one-dimensional case, then, the source must be injecting a concentration of N_0 particles per x_0 in each period of time of t_0 . Again, as in all cases of Fickian diffusion (defined by Eq. 5), the diffusion is determined by a single parameter $x/\sqrt{4Dt}$.

Fig. 6 represents the time evolution of the constant source diffusion at fixed points. As before, we note that the $1/e$ point of the concentration moves outward from the source at a linear rate of $\sqrt{4Dt}$, that is, for a diffusion constant of 7 cm^2/s , the $1/e$ point will be at about 3 m from the source point at hour later. For such diffusion rates, the sampling rates (10 ms) that we have available are more than adequate for resolving the shape of a rise in concentration. Even taking into account the five minute settling time associated with dissolved oxygen, the five element sensor will not miss a peak due to under sampling. The detection problem becomes one of sensitivity and accuracy. The diffusants are being distributed over three rather macroscopic dimensions. Even for a constant source, the dimensions of interest (tens to thousands of meters) require a significant amount of diffusant to be injected over a significant amount of time as we will see in the next section.

6 DISCUSSION

In order to use an array of sensors such as we have described for FEW management, specifically, to determine the coupling

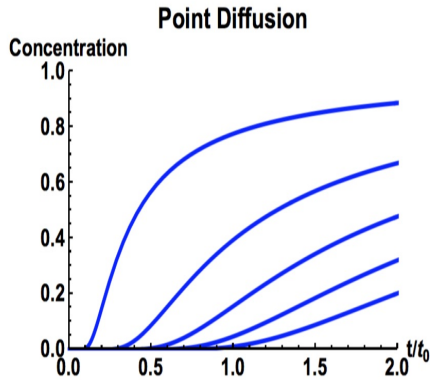


Figure 6: Time evolution of diffusant concentration at five different fixed distances from the point at which a constant diffusant source is applied. The distances to the observation point along the x/x_0 axis are given by $x/x_0=0.2, 0.6, 1.0, 1.4$ and 1.8 from the sharpest to the smoothest distribution.

between systems, we have assumed it is sufficient to identify and locate system stressors. Certainly, this has to be done rapidly enough that the information can be passed to management controller for the complete FEW system as soon as it is detected. From the above presentation, it should be clear that we can obtain the spatial and temporal resolution necessary to do this. That is, we can determine the source locations of all of the quantities that we sense with our archetypical sensor pack given that enough diffusant was deposited by the source to be above the sensitivity threshold and that currents in the surface water do not have a deleterious effect on the detection threshold. Let's take up sensitivity first.

We note that the $1/e$ point of the distributions Figs. 3 and `reffig:csd(x)` move outward such that at a time t_0 the $1/e$ point shows up at x_0 . We have also noted that the diffusion rates are circa $10 \text{ cm}^2/\text{s}$. We note that the sensitivity of our nitrate sensor is about 3% on the average value of 7 mg/liter . The minimum detectable change then must be circa 0.02 mg/l . For constant source diffusion, the value obtained at a very point will eventually be the same, that is, when we are injecting matter at the same rate that it is diffusing away from the injection point. Eventually, the value at the source point will reach a distant field point if the source is on for the time taken to diffuse to that point. With a diffusion constant of $6.25 \text{ cm}^2/\text{s}$, $(4Dt)^{3/2}$ equals 1000 cm^3 in roughly 2 seconds. If the source then were injecting $10 \mu\text{g/s}$, this stressor would be just barely seen at time t_0 later at a coordinate x_0 from the source. Similar considerations can be applied to other diffusants. This constant source case is a limiting case.

If we take the diffusion constant to be $D=7 \text{ cm}^2/\text{s}$, we note that the edge of the distribution moves about 3 m per hour. This is tiny compared the speed of river currents. For example, rivers such as the Amazon, the Mississippi and Nile

all have flow rates in excess of circa 1.5 m/s. The diffusion along a stream line will be totally unobservable but lateral rate of diffusion will be noticeable after some length. At 3 m per hour diffusion, one would only note about 1 m of lateral diffusion per km of flow along a 1.5 m/s current. Indeed, this is the reason why that at the junctions of rivers that carry different suspensions of silt with different colors, the individual rivers may keep their individual colors for many kilometers downstream. The most economical way to measure such spreading would be to have a much greater spacing of the sensors along the flow than transverse to the flow. If a sensor array with elements such as is described in this paper were to be deployed in a river with 1 m/s flow rate, a good strategy would be to place sensor elements a m apart transversely but a km apart longitudinally.

7 SUMMARY

To summarize, autonomous multi-element water quality sensors can be constructed with off-the-shelf elements using commercially available micro-processors, here, the micro-Arduino. Calibration data can be used to indicate which of the multitude of available sensors can and should be used in such a sensor pack in order to maximize battery life. Analysis shows that one can apply an array of such sensors to the problem of determination of location and temporal signature of stressors in a coupled food, energy and water system. Consideration such as advection versus diffusion can inform decisions concerning array construction.

REFERENCES

- [1] 1996. Water Quality Monitoring - A practical Guide to the Design and Implementation of Freshwater Quality Studies and Monitoring Programmes. (1996), 348 pages.
- [2] Erhan Alparslan, Gonca Coskun, and Ugur Alganci. 2009,9. Water quality determination of Küçükçekmece Lake, Turkey by using multispectral satellite data. *The Scientific World Journal* (2009,9), 1215–29.
- [3] Seongjoon Byeon, Gyewoon Choi, Seungjin Maeng, and Philippe Gourbesville. 2015. Sustainable Water Distribution Strategy with Smart Water Grid. *Sustainability (Switzerland)* 7,4 (2015), 4240 – 4259.
- [4] J. V. Capella, a. Bonastre, R. Ors, and M. Peris. 2010. A Wireless Sensor Network approach for distributed in-line chemical analysis of water. *Talanta* 80,5 (2010), 1789–1798.
- [5] Ni-Bin Chang, Sanaz Imen, and Benjamin Hannah. 2015. Remote Sensing for Monitoring Surface Water Quality Statan15,us and Ecosystem State in Relation to the Nutrient Cycle: A 40-Year Perspective. *Critical Reviews in Environmental Science and Technology* 45 (2015), 101–166.
- [6] Ni-Bin Chang, Sanaz Imen, and Benjamin Vannah. 2014. Remote Sensing for Monitoring Surface Water Quality Status and Ecosystem State in Relation to the Nutrient Cycle: a 40-year Perspective. *Critical Reviews in Environmental Science and Technology* 3389, July 2015 (2014).
- [7] Ni Bin Chang, Zhemin Xuan, and Brent Wimberly. 2012. Remote sensing spatiotemporal assessment of nitrogen concentrations in Tampa bay, Florida due to a drought. *Terrestrial, Atmospheric and Oceanic Sciences* 23, 5 (2012), 467–479.
- [8] Yirgalem Chebul, Ghinwa M. Naja, Rosanna G. Rivero, and Assefa M. Melesse. 2012. Water Quality Monitoring Using Remote Sensing and an Artificial Neural Network. *Water, Air, & Soil Pollution* 223,8 (2012), 4875–4887.
- [9] J. E. Cloern. 2001. Our evolving conceptual model of the coastal eutrophication problem. *Marine Ecology Progress Series* 210 (2001), 223–253.

- [10] Abel Rodriguez de la Conception, Riccardo Stefanelli, and Daniele Trinchero. October 10-13 2014. A Wireless Sensor Network Platform Optimized for Assisted Sustainable Agriculture. In *Proceedings of the IEEE Global Humanitarian Technology Conference (GHTC 14)*. 159 – 165.
- [11] Ziqian Dong, Fang Li, Babak Beheshti, Alan Mickelson, Marta Panero, and Nada Anid. 2016. Autonomous Real-time Water Quality Sensing as an Alternative to Conventional Monitoring to Improve the Detection of Food, Energy and Water Indicators. *Journal of Environmental Studies and Sciences* 6 (2016), 200–207.
- [12] Angel Miguel Villegas Erazo, Seok Yee Tang, and Yi Qian. 2006. Wireless Sensor Network Communication Architecture for Wide-Area Large Scale Soil Moisture Estimation and Wetlands Monitoring. *Walsip Research Project: Technical Report TR-NCIG-0501* (2006), 24.
- [13] Etimad Fadel, V. C. Gungor, Laila Nassem, Nadine Akkari, M. G. Abbas Maik, Suleiman Almasri, and Ian F. Akyildiz. 2015. A Survey of Wireless Sensor Networks for Smart Grid. *Computer Communications* 71 (2015), 22–33.
- [14] John W. Finley and James N. Seiber. 2014. The nexus of food, energy, and water. *Journal of Agricultural and Food Chemistry* 62, 27 (2014), 6255–6262.
- [15] Peter Fox-Penner. 2014. *Smart Power Anniversary Edition: Climate Change, The Smart Grid and the Future of Electric Utilities, Second Edition*. Island Press.
- [16] Jose Antonio Dominguez Gomez, Covadonga Alonso Alonso, and Ana Alonso Garcia. 2011. Remote sensing as a tool for monitoring water quality parameters for Mediterranean Lakes of European Union water framework directive (WFD) and as a system of surveillance of cyanobacterial harmful algae blooms (SCyanoHABs). *Environmental Monitoring and Assessment* 181, 1-4 (2011), 317–334.
- [17] Helen P Jarvie, Andrew N Sharpley, Don Flaten, Peter J a Kleinman, Alan Jenkins, and Tarra Simmons. 2015. The Pivotal Role of Phosphorus in a Resilient Water-Energy-Food Security Nexus. *Journal of Environmental Quality* 44, 4 (2015), 1049–1062.
- [18] Cary W. King and Michael Carabajales-Dale. 2016. Food-Energy-Water Metrics Across Scales: Project to System Level. *Journal of Environmental Studies and Science* 6 (2016), 39–49.
- [19] Victor Klemas. 2013. Remote sensing of emergent and submerged wetlands: an overview. *International Journal of Remote Sensing* 34,18 (2013), 6286–6320.
- [20] A. Kumar, M. O. Arshad, S. Mathavan, K. Kamal, and T. Vadamala. October 10-13 2014. Smart Irrigation Using Low-Cost Moisture Sensors and XBee-Based Communication. In *Proceedings of the IEEE Global Humanitarian Technology Conference (GHTC 14)*. 333 – 337.
- [21] Mathew Kurian and Reza Ardakanian. 2015. Governing the nexus: Water, soil and waste resources considering global change. *Governing the Nexus: Water, Soil and Waste Resources Considering Global Change* (2015), 1–230.
- [22] Abdulazeez T. Las and Samuel B. Adelaju. 2013. Progress and recent advances in phosphate sensors: A review. *Talanta* 114 (2013), 191–203.
- [23] Eunhyoung Lee, Sanghoon Han, and Hyunook Kim. January, 2013. Development of software sensors for determining total phosphorus and total nitrogen in waters. *International journal of environmental research and public health* 10,1 (January, 2013), 219–36.
- [24] Bruce E. Logan. 2015. Urgency at the Nexus of Food, Energy and Water Systems. *Environmental Letters* 2 (2015), 149–150.
- [25] Alan Mickelson and Daniel Tsvankin. 2017 in press. Information Systems for Real-Time Water Quality Monitoring. In *Encyclopedia of Sustainable Technology*, Martin Abraham (Ed.). Elsevier.
- [26] Alan Mickelson and Daniel Tsvankin. 2017 under review. Water Quality Monitoring for Coupled Food, Energy and Water (FEW) Systems. *Environmental Progress and Sustainable Energy* (2017 under review). Issue Special Issue on the FEW Nexus.
- [27] Michele Mutchek and Eric Williams. 2014. Moving Towards Sustainable and Resilient Smart Water Grids. *Challenges* 5 (2014), 123 – 137.
- [28] B. O'Flynn, Rafael Martinez-Catala, S. Harte, C. O'Mathuna, John Cleary, C. Slater, F. Reagan, D. Diamond, and Heather Murphy. 2007. Smart Coast: A Wireless Sensor Network for Water Quality Monitoring. In *Proceedings of the 32nd IEEE Conference on Local Computer Networks*. 815 – 816.
- [29] B O'Flynn, F Regan, A Lawlor, J Wallace, J Torres, and C O'Mathuna. 2010. Experiences and recommendations in deploying a real-time, water quality monitoring system. *Measurement Science and Technology* 21, 12 (2010), 124004.
- [30] Christie Ritter, Mallory Cottingham, Jared Leventhal, and Alan Mickelson. 2014. Remote Delay Tolerant Water Quality Monitoring. In *Proceedings of the 2014 Global Humanitarian Technology Conference*. 462–468.
- [31] Florina Ungureanu, Robert Gabriel Lupu, Andrei Stan, Ioan Craciun, and Carmen Teodosiu. 2010. Towards Real Time Monitoring of Water Quality in River Basins. *Environmental Engineering and Management Journal* 9, 9 (2010), 232430.
- [32] B. van de Kerkhof, M. van Persie, H. Noorbergen, L. Schouten, and R. Ghauharali. 2015. Spatio-temporal Analysis of Remote Sensing and Field Measurements for Smart Farming. *Procedia Environmental Sciences* 27 (2015), 21–25.
- [33] B. van de Kerkhof, M. van Persie, H. Noorbergen, L. Schouten, and R. Ghauharali. 2015. Spatio-temporal Analysis of Remote Sensing and Field Measurements for Smart Farming. *Procedia Environmental Sciences* 27 (2015), 21–25.
- [34] Christopher Warwick, Antonio Guerreiro, and Ana Soares. 2013. Sensing and analysis of soluble phosphates in environmental samples: A review. *Biosensors and Bioelectronics* 41,1 (2013), 1–11.
- [35] Chunfa Wu, Jiaping Wu, Jiaguo Qi, Lisu Zhang, Huiqing Huang, Liping Lou, and Yingxu Chen. 2010. Empirical estimation of total phosphorus concentration in the mainstream of the Qiantang River in China using Landsat TM data. *International Journal of Remote Sensing* 31 (2010), 2309–2324.
- [36] Sungwook Yoon and Hyenki Kim. 2014. Design and Implementation of Mobile Integration System for Smart Farming. *International Journal of Multimedia and Ubiquitous Engineering* 9(10) (2014), 223–230.
- [37] Marco Zennaro. 2010. *Wireless Sensor Networks for Development: Potentials and Open Issues*. Ph.D. Dissertation. KTH, School of Information and Communication Technology (ICT).
- [38] Marco Zennaro, Antoine Bagula, and Mayamiko Nkoloma. 2012. From Training to Projects: Wireless Sensor Networks in Africa. In *Proceedings of the Global Humanitarian Technology Conference (GHTC) 2012*. 417– 422.
- [39] Marco Zennaro, Athanasios Floros, Gotham Dogan, Tao Sun, Zhichao Cao, Chen Huang, Manzoor Bahader, Herve Ntareme, and Antoine Bagula. September 22 - 25, 2009. On the Design of a Water Quality Wireless Sensor Network (WQWSN): an Application in Water Quality Monitoring in Malawi. In *Proceedings of the IEEE Conference on Parallel Processing Workshops (ICPPW 09)*. 330 – 336.
- [40] M. Zennaro, H. Ntareme, and A. Bagula. 2008. Experimental Evaluation of Temporal and Energy Characteristics of an Outdoor Sensor Network. In *Mobility Conference 2008 - The International Conference of Mobile Technology, Applications and Systems*.
- [41] Lihua Zheng, Minzan Li, Caicong Wu, Haijian Ye, Ronghua Ji, Xiaolei Deng, Yanshuang Che, Cheng Fu, and Wei Guo. 2011. Development of a Smart Mobile Farming Service. *Mathematical and Computer Modelling* 54, 3-4 (2011), 1194–1203.
- [42] Serge Zhuiykov. 2012. Solid-state sensors monitoring parameters of water quality for the next generation of wireless sensor networks. *Sensors and Actuators, B: Chemical* 161,1 (2012), 1–20.
- [43] Huma Zia, Nick R. Harris, and Geoff Merrett. 2014. Water Quality Monitoring, Control and Management (WQMCM) Framework Using Collaborative Wireless Sensory Networks. In *Proceedings of 11th International Conference on Hydroinformatics (HIC 2014)*.
- [44] Huma Zia, Nick R. Harris, Geoff V. Merrett, Mark Rivers, and Neil Coles. 2013. The impact of agricultural activities on water quality: A case for collaborative catchment-scale management using integrated wireless sensor networks. *Computers and Electronics in Agriculture* 96 (2013), 126–138.